Müller Cell Ca^{2+} Waves Evoked by Purinergic Receptor Agonists in Slices of Rat Retina

YANG LI, LYNNE A. HOLTZCLAW, AND JAMES T. RUSSELL
Laboratory of Cellular and Molecular Neurophysiology, National Institute of Child Health and Human Development, National Institutes of Health, Bethesda, Maryland 20892

Received 8 May 2000; accepted in final form 11 October 2000

Li, Yang, Lynne A. Holtzclaw, and James T. Russell. Müller cell Ca^{2+} waves evoked by purinergic receptor agonists in slices of rat retina. *J Neurophysiol* 85: 986–994, 2001. We have measured agonist evoked Ca^{2+} waves in Müller cells in situ within freshly isolated retinal slices. Using an eye cup dye loading procedure we were able to preferentially fill Müller glial cells in retinal slices with calcium green. Fluorescence microscopy revealed that bath perfusion of slices with purinergic agonists elicits Ca^{2+} waves in Müller cells, which propagate along their processes. These Ca^{2+} signals were insensitive to tetrodotoxin (TTX, 1.0 μM) pretreatment. Cells were readily identified as Müller cells by their unique morphology and by subsequent immunocytochemical labeling with glial fibrillary acidic protein antibodies. While cells never exhibited spontaneous Ca^{2+} oscillations, purinoreceptor agonists, ATP, 2 MeSATP, ADP, 2 MeSADP, and adenosine readily elicited Ca^{2+} waves. These waves persisted in the absence of $[Ca^{2+}]_o$ but were abolished by thapsigargin pretreatment, suggesting that the purinergic agonists tested act by releasing Ca^{2+} from intracellular Ca^{2+} stores. The rank order of potency of different purines and pyrimidines for inducing Ca^{2+} signals was 2 MeSATP = 2MeSADP > ADP > ATP $\gg$ $\alpha\beta$meATP = uridine triphosphate (UTP) > uridine diphosphate (UDP). The Ca^{2+} signals evoked by ATP, ADP, and 2 MeSATP were inhibited by reactive blue (100 μM) and suramin (200 μM), and the adenosine induced signals were abolished only by 3,7-dimethyl-1-propargylxanthine (200 μM) and not by 1,3-dipropyl-8-(2-amino-4-chlorophenyl)-xanthine) or 8-cyclopentyl-1,3-dipropylxanthine at the same concentration. Based on these pharmacological characteristics and the dose-response relationships for ATP, 2 MeSATP, 2 MeSADP, ADP, and adenosine, we concluded that Müller cells express the P1A2 and $P2Y_1$ subtypes of purinoceptors. Analysis of Ca^{2+} responses showed that, similar to glial cells in culture, wave propagation occurred by regenerative amplification at specialized Ca^{2+} release sites (wave amplification sites), where the rate of Ca^{2+} release was significantly enhanced. These data suggest that Müller cells in the retina may participate in signaling, and this may serve as an extra-neuronal signaling pathway.

INTRODUCTION

Glial cells, like neurons, participate in signaling in the mammalian nervous system. Glial cells monitor and respond to neuronal activity and transmit such activity over long distances by way of propagating Ca^{2+} waves (Smith 1992). Moreover, bi-directional glial-neuronal communication has received increasing attention as a potential mode of cell-cell signaling in the CNS (Dani et al. 1992; Duffy and MacVicar 1995; Grosche et al. 1999; Mennerick and Zorumski 1994; Nedergaard 1994; Newman and Zahs 1997; Pasti et al. 1997; Porter and McCarthy 1996; Wu and Barish 1994). Propagation of Ca^{2+} waves through a network of intercommunicating astrocytic processes in the CNS could serve as a conduit for extraneuronal, long-distance intercellular communication. The cellular mechanisms that support the temporal and spatial characteristics of such glial Ca^{2+} waves in situ, however, are not fully understood. We have recently shown that in glial cells in culture, Ca^{2+} wave propagation in processes occurs by regenerative Ca^{2+} release at specialized release sites or "wave amplification sites" (Simpson and Russell 1998; Simpson et al. 1997; Yagodin et al. 1994). It remains to be seen whether these observations in cultured cells reflect glial responses in situ.

Müller cells, the principal glial cells in the retina, provide an ideal experimental model to study the cell biology of wave propagation. These cells span almost the entire depth of the retina from the outer photoreceptor layer to the inner border of the retina, where they terminate in expanded end-feet adjacent to the vitreous humor (see review by Newman and Reichenbach 1996). Müller cells have long, relatively linear processes, which allows for precise analysis of Ca^{2+} wave propagation. To utilize their unique morphology, we developed a novel dye loading method in the eyecup, in which Müller cells are preferentially filled with calcium green. Wave propagation in identified single Müller cells was recorded using a conventional wide-angle fluorescence microscope.

The goals of this study were as follows: *1*) to investigate whether the cellular mechanism of Ca^{2+} wave propagation in situ mirrors that described in cultured glial cells, *2*) to describe the temporal and spatial characteristics of Ca^{2+} wave propagation within Müller cells in intact retinal slices, and *3*) to characterize receptor systems that evoke Ca^{2+} waves in Müller cells. Although Ca^{2+} waves between Müller cell end-feet have been recorded across the vitreal surface of flat-mounted whole retina (Newman and Zahs 1997), these waves were visualized by confocal microscopy in different optical sections through the thickness of the retina. In contrast, we studied wave propagation along single Müller cell processes to investigate the underlying cellular mechanisms that support intracellular Ca^{2+} waves. We prepared slices of retina where the Müller cells were discretely loaded with the Ca^{2+} indicator dye, calcium

Address for reprint requests: J. T. Russell, Laboratory of Cellular and Molecular Neurophysiology, NICHD, NIH, Bldg. 49, Rm. 5A-78, Bethesda, MD 20892 (E-mail: james@helix.nih.gov).

The costs of publication of this article were defrayed in part by the payment of page charges. The article must therefore be hereby marked "*advertisement*" in accordance with 18 U.S.C. Section 1734 solely to indicate this fact.

green, and recorded Ca^{2+} waves through the entire length of processes in the plane of the microscopic field using fluorescence microscopy. We show that Ca^{2+} waves in Müller cells are elicited by purinergic activation. In addition, like in cultured glial cells, Müller cell waves propagate by regenerative Ca^{2+} release at a series of wave amplification sites along the length of processes.

METHODS

Indicator loading

Müller cells in the adult rat retina were selectively loaded with the Ca^{2+} indicator dye, calcium green, using an eyecup loading technique. Retinae were isolated from male Sprague Dawley rats maintained under a 12-h light-dark cycle using procedures authorized by the Animal Use and Care Committee, National Institute of Child Health and Human Development, National Institutes of Health (protocol number 98-017). Following decapitation, the eye lid and other connective tissue covering the eye were peeled away, and the eye was gently rolled out of the socket and transferred to a dish with fresh artificial cerebral spinal fluid (ACSF; in mM: 117.4 NaCl, 2.0 KCl, 1.4 $MgSO_4$, 2.5 $CaCl_2$, 1.0 KH_2PO_4, 26.2 $NaHCO_3$, and 11.0 glucose), which was continuously aerated with 95% O_2 containing 5% CO_2. The anterior chamber of the eye was opened, and the iris, lens, and vitreous humor were removed. To make a useful eyecup for subsequent dye loading, it was essential to cut and trim the tissue above the ora serrata, since the retina was firmly attached to the pigment epithelium in only two areas, the optic disk and the ora serrata. The isolated eyecup was placed in ACSF containing collagenase (2 mg/ml) and DNase (0.1 mg/ml) and incubated at 30°C for 15 min to ensure complete removal of the remaining vitreous humor. This treatment improved dye access to the Müller cell endfeet (Coleman and Miller 1989; Gottesman and Miller 1992; Newman and Zahs 1997). The eyecup was then incubated for 2 h at 30°C in oxygenated ACSF containing calcium green AM (70 μg/ml; Molecular Probes) dissolved in DMSO containing pluronic acid (4.7 mg/ml). At this stage the retina was intact ensuring that only Müller cell end feet were exposed to indicator containing solution. This precaution prevented cells other than Müller cells such as astrocytes from taking up the dye. Retinae were then isolated from the eyecup, laid photoreceptor layer down, and chopped into 100-μm slices using a McIlwain tissue chopper. Slices were submerged immediately in oxygenated ACSF and maintained in the dark at room temperature. Slices were used within 4–5 h after loading.

Solution perfusion and drugs

Dye-loaded retinal slices were transferred to a Leiden cover slip chamber and secured with specimen grips and a metal weight. Slices were submerged in ACSF and continuously aerated with 95% O_2 in 5% CO_2. The volume of the recording chamber was approximately 0.3 ml. Slices were perfused at the rate of 2.5 ml/min. The drugs used were disodium ATP, tetrodotoxin, 2 MeSATP, 2 MeSADP (RBI), uridine triphosphate (UTP), phenylephrine, and glutamate and reactive blue (Sigma Chemical), suramin, (Calbiochem), and thapsigargin (LC Service).

$[Ca^{2+}]_i$ measurements and data analysis

Calcium green fluorescence was imaged with an inverted microscope on a vertical optical bench using a Nikon ×40/1.3 NA CF Fluor DL objective lens. The slice preparation was illuminated with a mercury arc lamp (Oriel Optics), with quartz collector lenses. A shutter (Uniblitz), an excitation filter (495 nm), appropriate dichroic mirror, and a long pass filter (515 nm) were mounted in the light path such that fluorescence could be imaged through a microchannel plate intensifier (Model KS-1380, Videoscope International, Washington, DC) using a charge-coupled device (CCD) camera (Pulnix). Images were digitized and integrated (2 frames per image) on a Macintosh computer running Synapse, an image acquisition and analysis program (Synergy Research, Silver Spring, MD). The time interval between images varied depending on the required temporal resolution and ranged from 2 to 30 images/s. After all the images were acquired, Müller cells were outlined with a region of interest (ROI) tool, and fluorescence intensity within the whole cell or sub-regions of cells was extracted and analyzed. Wave propagation and local Ca^{2+} release rates were analyzed in consecutive cellular sections as described previously (Simpson et al. 1997; Yagodin et al. 1994). Images of Müller cell processes were divided for analysis into 0.8- to 2.0-μm-wide regions sequentially along the longitudinal axis, and fluorescence intensity values in the nonzero pixels within each slice were averaged (F) and plotted as normalized fluorescence intensities ($\Delta F/F_0$) against time.

Immunohistochemistry

In some experiments, cells were verified as Müller cells by immunocytochemistry using antibodies against glial fibrillary acidic protein (GFAP). Immediately following a recording, retinal slices were fixed in 4% paraformaldehyde for 30 min, and then rinsed in PBS (pH 7.3). The fixed sections were then permeabilized and blocked in PBS containing 0.3% Triton X-100, 1% BSA, and 20% normal goat serum (pH 7.4) for 1 h at room temperature. The sections were then incubated in anti-GFAP antibody (Boehringer Mannheim) for 18 h at 4°C in the same solution as above, but containing 1% normal goat serum. Sections were washed extensively in PBS and incubated with a fluorescence-conjugated goat anti-mouse antibody for 90 min and then washed again. After a brief PBS rinse, the sections were dried and mounted with Mowiol onto gelatin-coated glass slides. Cells were imaged using a fluorescence microscope with a digital cooled CCD camera (Photometrics, Tucson, AZ).

RESULTS

Specific labeling of Müller cells in retinal slices

Fluorescent indicator dyes were preferentially taken up by Müller cells by the use of the eyecup loading technique. Müller cells were easily distinguished within the tissue by their intense fluorescence signal and elongated bipolar morphology, which spanned the entire thickness of the retinal slice (Fig. 1). The end-feet and the soma appeared intensely fluorescent compared with the processes (Fig. 1*B*). To examine cellular morphology in detail, Müller cells were loaded with calcein using the same eyecup loading procedure. Calcein-loaded Müller cell processes appeared regular with very fine hairlike branches (Fig. 1*A*). In some experiments, calcium green–loaded Müller cells were identified by subsequent immunohistochemistry using anti-GFAP antibodies. Figure 1*C* shows one example where Müller cells in a retinal slice were labeled immunocytochemically following $[Ca^{2+}]_i$ measurements and were identified as GFAP-positive glial cells. Examination under confocal optics revealed that only Müller glial cells were loaded with calcium green as no fluorescence was detected in astrocytes or ganglion cells (data not shown). Thus all the fluorescence measured in

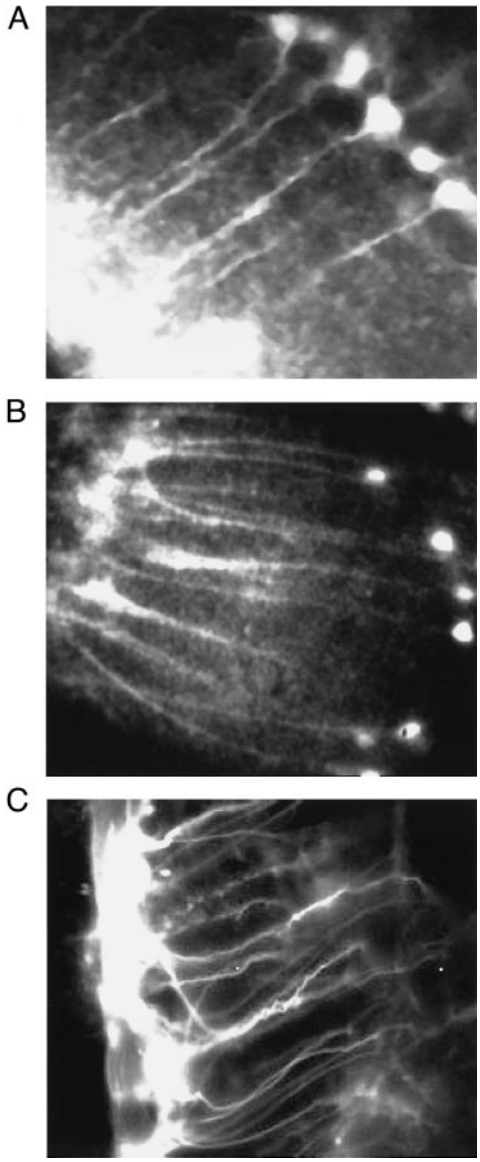

FIG. 1. Identification of dye-loaded cells as Müller cells. *A*: image of a retinal slice loaded with calcein. Dye loading was carried out in the eyecup as described in METHODS. Note only Müller cells are loaded. *B*: typical image of a calcium green–loaded retinal slice showing brightly fluorescent Müller cells. Müller cells were identified by their bipolar morphology, with processes extending from the end-feet at the internal limiting membrane to the external limiting membrane. The brightness and contrast settings in the image were chosen to highlight the Müller cell processes, which saturated the end-feet and cell body regions. No fluorescence was observed in astrocytes or ganglion cells. *C*: glial fibrillary acidic protein (GFAP)–containing Müller cells visualized by fluorescence-based immunocytochemistry using specific anti-GFAP antibodies. This retinal slice was incubated with antibodies following measurement of $[Ca^{2+}]_i$ signals. Cells loaded with calcium green were also positive for GFAP. Note that GFAP immunoreactivity does not extend into the expanded end-feet (*C*).

our experiments originated from within Müller cells. Damaged preparations, where fluorescence was observed within astrocytes and neurons (<15% of retinae) were routinely discarded.

Purinergic receptor–mediated $[Ca^{2+}]_i$ transients in Müller cells

In the absence of stimulation, Müller cells in retinal slices did not show spontaneous $[Ca^{2+}]_i$ changes. Bath application of

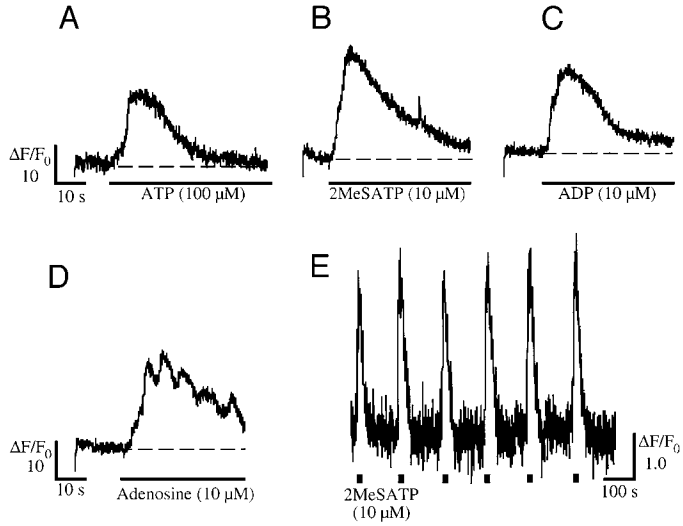

FIG. 2. Purinergic agonists evoke $[Ca^{2+}]_i$ increase in Müller cells in situ. Retinal slices were placed on the microscope stage in a Leiden coverslip chamber and were continuously perfused with artificial cerebrospinal fluid (ACSF). Calcium green fluorescence was imaged in a wide-angle fluorescence microscope. Slices were perfused with different purinergic agonists as indicated by black bars underneath each trace. Traces show normalized ($\Delta F/F_0$) fluorescence intensities within the entire cell image plotted against time. *A*: ATP, 100 μM. *B*: 2 MeSATP, 10 μM. *C*: ADP, 10 μM. *D*: adenosine, 10 μM. *E*: repeatable responses to brief (15 s) perfusions with 2 MeSATP.

purinergic agonists, however, increased $[Ca^{2+}]_i$ in all the Müller cells examined as indicated by the increase in calcium green fluorescence (Fig. 2). The P2 purinoreceptor agonists, ATP (100 μM, Fig. 2*A*), 2-methylthio-ATP (2 MeSATP, 10 μM, Fig. 2*B*), ADP (10 μM, Fig. 2*C*), and the P1 receptor agonist adenosine (10 μM, Fig. 2*D*) all elicited $[Ca^{2+}]_i$ rises. The pattern of these responses consisted of an initial rapid rise to peak within 5 to 10 s of agonist application, followed by a slow decline to a plateau level higher than the prestimulus level of $[Ca^{2+}]_i$ (Fig. 2, *A–D*). Rarely did the fluorescence signal decline to prestimulus levels in the presence of agonist, but on removal of agonist it promptly returned to resting levels. In many instances (25 of 44 cells), oscillatory changes in $[Ca^{2+}]_i$ were observed when slices were perfused with adenosine (Fig. 2*D*). Brief (15 s) applications of 2 MeSATP elicited repeated $[Ca^{2+}]_i$ transients of reduced amplitude, which remained constant over a number of trials (Fig. 2*E*). Similar results were obtained in 35 separate slices (140 cells), and the results are compiled in Table 1. These purinergic receptor–mediated $[Ca^{2+}]_i$ signals were most likely due to direct stimulation of

TABLE 1. *Pharmacological characterization of purinergic receptor in retinal Müller cells in situ*

	Responding Cells, %	Peak Amplitude ($\Delta F/F_0$)	*n*
ATP	100	14.60 ± 1.10	51
2MeSATP	100	18.30 ± 0.95	71
Adenosine	80	10.16 ± 1.07	44
ADP	97	16.21 ± 1.13	33
$\alpha\beta$MeATP	41	4.12 ± 0.38	25
UTP	36	4.91 ± 0.94	11
UDP	8	4.42 ± 0.58	3

Values in Peak Amplitude are means ± SE; *n* is number of cells. UTP, uridine triphosphate; UDP, uridine diphosphate.

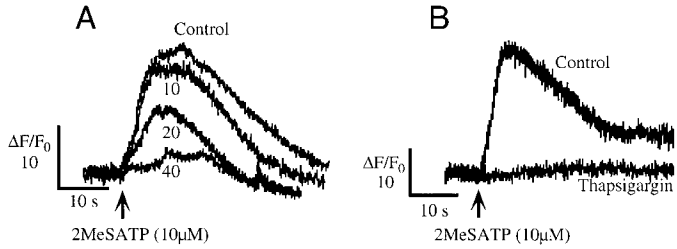

FIG. 3. Dependence of purinoceptor responses on extracellular vs. intracellular Ca^{2+} stores. *A*: retinal slices were perfused with normal ACSF or Ca^{2+}-free ACSF containing EGTA (100 μM) for indicated periods of time prior to stimulation with 2 MeSATP. Traces show $[Ca^{2+}]_i$ responses in representative cells in normal ACSF and following 10-, 20-, and 40-min perfusion with Ca^{2+}-free ACSF. *B*: slices were treated with thapsigargin (5 μM) for 15 min and then stimulated with 2 MeSATP. Traces show response to 2 MeSATP before (control) and after thapsigargin treatment.

Müller cells as the responses were unaffected by blocking neuronal stimulation and action potential propagation by pretreatment of slices with TTX (1 μM, 4 slices).

While all the cells responded to ATP or 2 MeSATP, very few of the cells responded to norepinephrine or glutamate. Norepinephrine (500 μM)-induced Ca^{2+} responses were observed only in two of six retinal slices, while all cells in the field of view in the same six slices showed Ca^{2+} rises in response to ATP (10 μM) and 2 MeSATP (1 μM). In contrast to findings in freshly isolated Müller cells (Keirstead and Miller 1995, 1997), application of glutamate (up to 1 mM) had little effect on Müller cells in situ in retinal slices (15 cells in 3 slices).

Müller cell $[Ca^{2+}]_i$ signals are due to Ca^{2+} release from cellular stores

To test whether the presence of extracellular Ca^{2+} is required for purinergic receptor–evoked $[Ca^{2+}]_i$ signals, we replaced normal ACSF with medium containing zero Ca^{2+} and 100 μM EGTA. We found that removal of extracellular Ca^{2+} over short periods of time (up to 10 min of perfusion) did not significantly alter either the amplitude or the pattern of 2 MeSATP–evoked responses (Fig. 3*A*). Prolonged incubation in Ca^{2+}-free medium with repeated agonist stimulations, however, resulted in the loss of response, probably due to complete depletion of the intracellular Ca^{2+} stores (Fig. 3*A*).

In another set of experiments, intracellular Ca^{2+} stores were depleted with thapsigargin, which inhibits the sarcoendoplasmic reticulum Ca^{2+} ATPase and thus depletes the endoplasmic reticulum Ca^{2+} stores in cells (Thastrup 1990). A 15-min perfusion with thapsigargin (5 μM) abolished all $[Ca^{2+}]_i$ responses to ATP or 2 MeSATP (Fig. 3*B*). Taken together, these results show that the Müller cell $[Ca^{2+}]_i$ responses to ATP and 2 MeSATP are due to Ca^{2+} release from intracellular stores rather than from an influx of extracellular Ca^{2+}. Newman and Zahs (1997) obtained similar results in their experiments on retinal whole-mount preparations.

Pharmacology of purinergic receptor–mediated $[Ca^{2+}]_i$ signals in Müller cells

Purinergic receptors have been classified into two major types. P1 adenosine receptors (subtypes A1 and A2) are G-protein–coupled receptors and act via phospholipase-C (Burnstock et al. 1983; Cusack and Hourani 1982). P2 purinergic receptors have two subtypes, ionotropic P2X receptors and metabotropic P2Y receptors, which like P1 receptors act via phospholipase-C. Seven different subtypes of P2Y receptors have been described based on the rank order of potency of different nucleotide agonists (see Burnstock 1997). Since the Müller cell $[Ca^{2+}]_i$ responses to ATP, 2 MeSATP, and adenosine were not abolished in the absence of $[Ca^{2+}]_o$, but were abolished by treatment with thapsigargin, we conclude that these responses are mediated by P2Y and P1 types of metabotropic purinoceptors. $\alpha\beta$-Methylene-ATP ($\alpha\beta$meATP, 1 μM), the known agonist for P2X subtype of receptors, produced small increases in $[Ca^{2+}]_i$ in <10% of Müller cells examined.

We systematically tested a number of agonists to determine the major purinoceptor subtype involved in the evoked $[Ca^{2+}]_i$ response in Müller cells. In these experiments, ATP was applied at the beginning and the end of each experiment, and only cells with comparable responses at the beginning and end were included in the analysis. Agonists were tested from low to high concentrations with a 15-min wash in between. Dose-response relationships were constructed for ATP, 2 MeSATP, 2 MeSADP (Fig. 4*A*), and ADP (Fig. 4*B*). The threshold concentrations were 1.0, 0.01, and 0.1 μM for ATP, 2 MeSATP, and ADP, respectively. The EC_{50} for the different nucleotides were (in μM), ATP, 7.0 $\pm$ 0.67; 2 MeSATP, 0.12 $\pm$ 0.06; 2 MeSADP, 0.22 $\pm$ 0.05; and ADP, 0.93 $\pm$ 0.03, showing that ADP, 2 MeSATP, and 2 MeSADP have 10-fold higher affinity for the receptor than ATP. These results are in general agreement with other reports (Burnstock et al. 1983; Cusack and Hourani 1982; Dixon 2000) and support the conclusion that the Müller cells in rat retina express P2Y purinoceptors and their stimulation results in a robust $[Ca^{2+}]_i$ response. Furthermore, in separate trials, the P2Y antagonists suramin (200 μM) and reactive blue (100 μM) both blocked the $[Ca^{2+}]_i$ responses in Müller cells evoked by ATP and 2 MeSATP (Fig. 5, *A–C*).

In addition, we also tested $\alpha\beta$MeATP, UTP, and uridine diphosphate (UDP) and found that the P2Y agonists, 2 MeSATP, 2 MeSADP, ADP, and ATP were by far the most potent and stimulated most Müller cells (Table 1). Only 36 and 8% of Müller cells responded to the P2 agonists UTP and UDP,

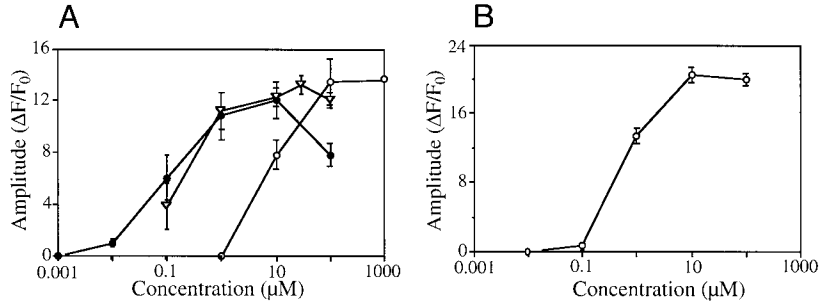

FIG. 4. Dose-response relationships. Data represent means $\pm$ SE of 8 separate measurements. Peak amplitudes ($\Delta F/F_0$) of evoked fluorescence increases were averaged and plotted against agonist concentration. ATP ($\circ$ in *A*), 2 MeSATP ($\bullet$ in *A*), 2 MeSADP ($\triangledown$ in *A*). *B*: concentration response relationship for ADP. The EC_{50} for the 3 agonists were (in μM) ATP, 7.0 $\pm$ 0.67 (n = 25); 2 MeSATP, 0.12 $\pm$ 0.06 (n = 30); 2 MeSADP, 0.22 $\pm$ 0.05; and ADP, 0.93 $\pm$ 0.03 (n = 12).

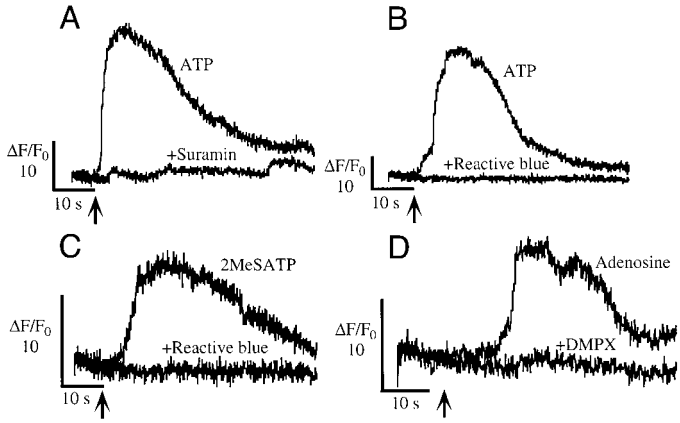

FIG. 5. Purinoceptor antagonists block Müller cell $[Ca^{2+}]_i$ transients. ATP-evoked Ca^{2+} transients were completely blocked by the P2 antagonists suramin (200 μM, *A*) and reactive blue (100 μM, *B*). Similarly, 2 MeSATP responses were blocked by reactive blue (100 μM, *C*). In *D*, $[Ca^{2+}]_i$ transients evoked by adenosine (10 μM) is blocked by 3,7-dimethyl-1-propargylxanthine (DMPX; 200 μM). Slices were perfused with antagonists for 5 min prior to agonist application.

respectively (Table 1). The rank order of potency for the purine and pyrimidine nucleotides was 2 MeSATP = 2 MeSADP > ADP > ATP $\gg$ $\alpha\beta$meATP = UTP > UDP. These results suggest that $P2Y_1$ subtype of receptors mediate the $[Ca^{2+}]_i$ signals evoked by the purinoceptor agonists in Müller cells. Adenosine was as potent as 2 MeSATP in eliciting Müller cell $[Ca^{2+}]_i$ responses (Table 1, Figs. 2*D* and 5*D*), suggesting that Müller cells also express P1 purinoceptors. To determine the adenosine receptor subtype (A1 or A2) involved, in separate experiments, we tested the selective A_1 antagonists 1,3-dipropyl-8-(2-amino-4-chlorophenyl)-xanthine (PAPCX) or 8-cyclopentyl-1,3-dipropylxanthine (DPCPX) or the selective A_2 antagonist 3,7-dimethyl-1-propargylxanthine (DMPX). Slices were stimulated with adenosine (10 μM) in the presence or absense of antagonists. We found that while PAPCX and DPCPX were totally ineffective in antagonizing the adenosine evoked $[Ca^{2+}]_i$ responses (5 trials, data not shown), DMPX (100 μM) completely abolished the responses in 10 separate trials (Fig. 5*D*). Taken together, these data suggest that in the retina, both intercellular communication and intracellular Ca^{2+} waves through the thickness of the retina within Müller cells could occur by a purinergic receptor–mediated mechanism.

Ca^{2+} wave propagation in individual Müller cells

To investigate the spatiotemporal characteristics of the Ca^{2+} signals in Müller cell processes, we acquired images rapidly (every 100 ms). Movies of image sets showing Ca^{2+} responses revealed that the signals always initiated in one region of Müller cells and propagated as waves through the processes. Figure 6 shows a montage of a series of images showing Ca^{2+} responses in a retinal slice stimulated with 2 MeSATP (10 μM). This representative image sequence shows a Ca^{2+} wave originating at the end-feet (*top* of picture) and propagating to the cell body (bright spots at the *middle* of the image) and then toward the photoreceptor layer at the *bottom* of the picture. In addition, bi-directional propagation of waves from a single initiation site was often observed (see Fig. 8), suggesting that diffusion of agonist across the slice does not determine the direction of the wave. Propagation of Ca^{2+} waves from one Müller cell to others can also be seen in the *bottom half* of the montage. Waves between cells were often observed, and the direction of propagation of these intercellular waves did not depend on the direction of fluid flow. We analyzed wave propagation through the cell body and the thin processes using digital image processing techniques (see Figs. 7 and 8).

Ca^{2+} wave propagation in situ was analyzed using paradigms developed in our laboratory to investigate propagation in cultured glial cells (Fig. 7) (Simpson et al. 1997; Yagodin et al. 1994). Cell images were sectioned into serial slices, and the average fluorescence intensity over time within each of these regions was plotted with an offset along the *Y*-axis (Fig. 7*B*). The offset plot shows that in this Müller cell, the very first Ca^{2+} wave initiated close to the end-foot and another one a little later near the photoreceptor layer and both waves propagated toward the cell body. To obtain quantitative estimates of wave speed and local Ca^{2+} release kinetics, the cell was sectioned into 0.85-μm-thick slices, and fluorescence intensity data were extracted from each slice. Peak amplitude, rate-of-rise, as well as the time at which 50% peak was reached were extracted from each trace and were plotted against cell length (Fig. 8) (see Simpson et al. 1997; Yagodin et al. 1994 for methods). For reasons of clarity only data from the end foot to the cell body region is shown in Fig. 8. This analysis revealed that the peak amplitude and rate of rise of the Ca^{2+} response were nonuniform through the cell, with some regions of the cell showing higher Ca^{2+} release rates than found in surrounding regions (arrows). At these sites, the local signal amplitude was higher (Fig. 8), and the rate of rise of the response was steeper (not shown). Thus the kinetic profile of these regions appeared similar to the specializations (wave amplification sites) previously observed in cultured glial cells (Simpson and Russell 1996; Yagodin et al. 1994).

A plot of the delay times to 50% peak of the signal against cell length localizes wave initiation sites in the cell. At these sites, the wave reaches 50% of maximum amplitude sooner than the surrounding regions and appears as minima in this plot (Fig. 8, ○). In this cell, the wave initiates at approximately 18 μm from the end-foot (∗). Wave speed was calculated from the slope of the line through the data points (Fig. 8). While the average wave speed was approximately 18 μm/s, waves slowed and sped up during propagation through different regions of the cell. Wave speed varied between 10 and 40 μm/s along processes. On average, waves took about 4–10 s to travel from end-feet to the cell body. From the initiation sites, waves propagated in both directions (see Fig. 8). In most of our experiments, waves initiated in the end-foot region of Müller cells and propagated toward the cell body. Of the 56 separate cells analyzed, 55% of waves initiated at the end-feet, 39% in the process region, and only in 5% of cells, waves initiated at the cell soma.

The peaks in Ca^{2+} release amplitude or the wave speed observed along Müller cell processes did not correspond to the peaks in the fluorescence intensity profile of the process (data not shown). This observation suggests that irregular process shape and thus variations in dye volume along processes do not contribute to the differences in Ca^{2+} release kinetics we measured. Such differences in fluorescence intensity along processes were corrected by the $\Delta F/F_0$ normalization procedure. Furthermore, transient dynamic changes in shape were never observed during purinergic stimulation, and plots of $\Delta F/F_0$ in

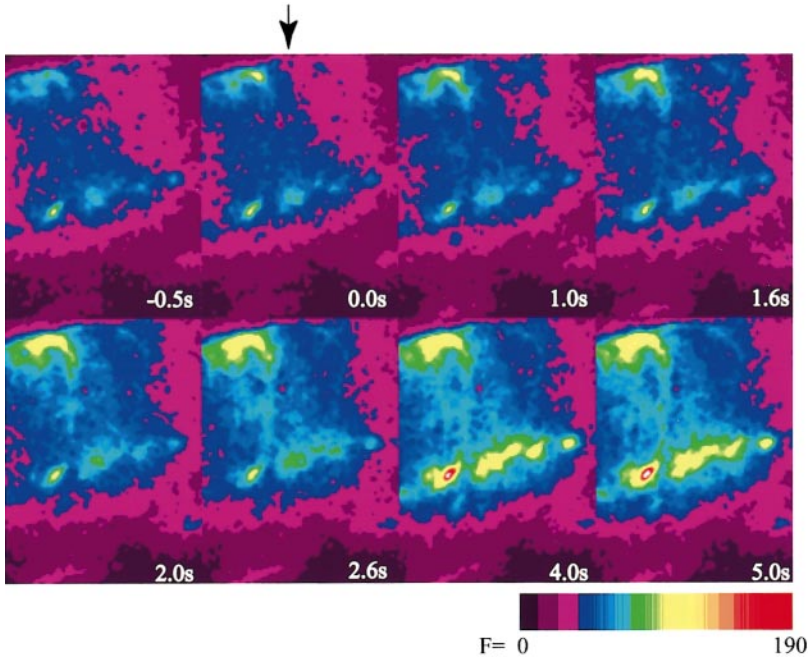

FIG. 6. Müller cell Ca^{2+} waves are evoked by 2 MeSATP. Montage of fluorescence images showing a 2 MeSATP–evoked Ca^{2+} wave in a retinal slice. Although ratio images were acquired every 200 ms, images representing specific time intervals were chosen to highlight wave propagation. Acquisition times are as noted in each panel where 0.0 s represents time of 2 MeSATP (10 μM) addition (arrow). A Ca^{2+} wave initiates at the end-foot region of one of the Müller cells in the field (middle of the field at the *top*), which propagates down toward the cell body and the photoreceptor layer at the *bottom*. Note also, waves propagating to other Müller cells, both at the end-feet region and the cell bodies. Fluorescence intensity in the 8-bit scale was rendered in pseudocolor as shown at *bottom right*. This qualitative view of wave propagation is better appreciated as a movie; see http://dir.nichd.nih.gov/Lcmn/RussellLab.

unstimulated processes did not show any peaks. Taken together, these data indicate that, like in cultured glial cells, Ca^{2+} wave propagation in Müller cells in situ is achieved through a series of wave amplification sites where the local Ca^{2+} release function is specialized.

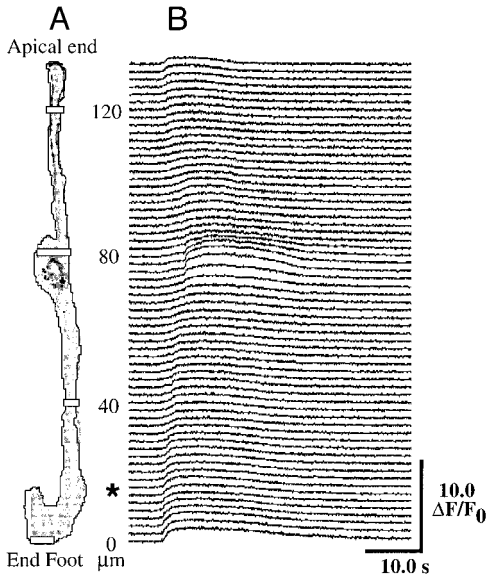

FIG. 7. Analysis of Müller cell Ca^{2+} waves. The data in the figure are from the same experiment depicted in Fig. 6 (cell in the *middle* of the panels). The agonist-evoked Ca^{2+} wave was analyzed by sectioning the Müller cell into 2.125-μm-wide (5 pixels) serial slices and measuring average fluorescence intensities within these regions of interest. *A*: a drawing of the analyzed cell and boxes marked within the cell outline indicate sections of the cell at 0, 40, 80, and 120 μm from the end-foot. *B*: normalized fluorescence intensity values ($\Delta F/F_0$) measured within such regions of interest were plotted with an offset on the *Y*-axis against time. The *bottom traces* on the figure correspond to responses from end-feet (0 μm) and *top traces* to the apical end of the cell. In this cell, the very 1st Ca^{2+} wave initiated near the end-foot and apical regions (*) and propagated toward the cell body. Note also another wave beginning a little later near the apical end (at ~110 μm).

DISCUSSION

In this study, we analyzed agonist-evoked Ca^{2+} wave propagation within Müller cell processes in slices of adult rat retinae. Using a novel indicator loading technique, we have discretely filled Müller cells with calcium green and measured Ca^{2+} transients evoked by bath-applied agonists. Immunocytochemical identification of cells using anti-GFAP antibodies clearly showed that the cells loaded with Ca^{2+} indicator were indeed Müller glial cells (Fig. 1). We found that purinergic agonists were very potent agents for eliciting Ca^{2+} responses

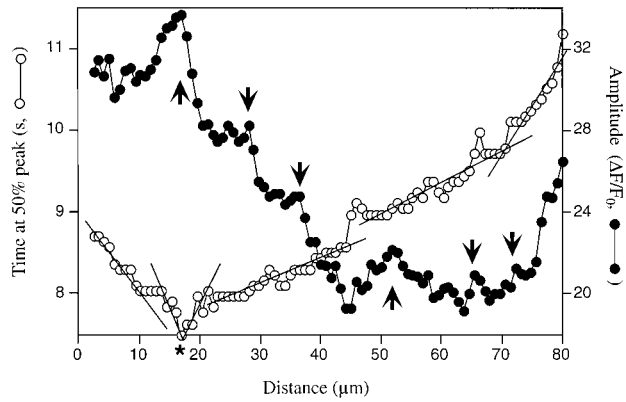

FIG. 8. Identification of specialized Ca^{2+} release sites. Data are from the same experiment shown in Figs. 6 and 7. For quantitative analysis the cell was sectioned into much finer 0.85-μm-wide slices. Parameters of local Ca^{2+} release kinetics, peak amplitude (●), and the time to 50% of peak (○) were extracted from each of the Ca^{2+} traces and were plotted against length of the cell. For the sake of clarity, only data from the end-foot to a distance of 80 μm into the cell (the cell body) are included in this plot. The amplitude of local Ca^{2+} release showed discrete peaks at a number of local cellular sites (arrows). Note also that the 1st wave initiation site (the minimum on the delay at 50% peak trace marked with an asterisk). Extrapolation (lines drawn through the points) of the delay at 50% peak provided estimates of wave speed and revealed that wave speed changes over the length of the cell.

in Müller cells. These Ca^{2+} responses initiated in specific regions of the Müller cell and propagated bi-directionally at nonuniform rates through cellular processes. There appeared to be specific cellular locations at which Ca^{2+} release rate and amplitude were significantly higher suggesting wave amplification sites.

Newman and Zahs (1997) have recently shown that in whole flat mount preparations of rat retina, exogenous addition of agonists as well as electrical stimulation can evoke Ca^{2+} waves that propagate between Müller cell end-feet. In addition, they showed that these Ca^{2+} waves modulate ganglion cell excitability (Newman and Zahs 1998). We were interested to know whether these Ca^{2+} waves impinge on signaling within the retina, specifically, do Ca^{2+} waves travel from the end-feet through the entire length of Müller cells to the photoreceptor layer of the retina. Our present study shows that Ca^{2+} waves propagate along Müller cell processes and this propagation occurs by regenerative Ca^{2+} release at specialized release sites along the processes. These results suggest that Müller cells may indeed act to modulate signaling throughout the thickness of the retina.

It was important to test whether the Müller cell Ca^{2+} responses are a direct consequence of stimulation of purinergic receptors on Müller cells or if the waves are due to indirect stimulation of Müller cells by synaptic release of transmitter resulting from purinergic stimulation of neural networks. We provide evidence that the responses are due to direct stimulation of Müller cells. Removal of Ca^{2+} from the bathing medium that blocks vesicular transmitter release (Llinas 1982) did not abolish the Ca^{2+} waves. Furthermore, blockade of action potentials with tetrodotoxin (TTX, 1.0 μM) did not inhibit the agonist-evoked Ca^{2+} signals. While it can be argued that under conditions of extracellular Ca^{2+} removal and TTX blockade, cellular signaling can occur through generation of graded potentials using surface charge effects; the more direct interpretation of our results is that purinergic agonists act directly on Müller cells. Finally, a graded dose-response relationship was obtained with increasing agonist concentrations, which further suggests that the primary Ca^{2+} response occur in Müller cells.

The fact that complete removal of Ca^{2+} from the bathing medium did not abolish Ca^{2+} waves, while depleting intracellular stores of Ca^{2+} did abolish waves, suggests that the ATP- and adenosine-evoked Müller cell Ca^{2+} waves were due to stimulation of metabotropic purinergic receptors, which include P2Y and P1 subtypes. Previous studies have resulted in classification of the P2Y purinoceptor subtypes using rank order of agonist potency (see for reviews Burnstock 1997; Dixon 2000; North and Barnard 1997). The rank order of potency in Müller cells in our experiments was 2 MeSATP = 2MeSADP > ADP > ATP $\gg$ $\alpha\beta$meATP = UTP > UDP, suggesting that Müller cells in rat retina express $P2Y_1$ subtype of purinergic receptors. Furthermore, since Ca^{2+} waves were also evoked by the P1 agonist, adenosine, and these waves were blocked by DMPX and not by PAPCX or DPCPX, we conclude that adenosine is acting via stimulation of $P1A_2$ purinergic receptors in Müller cells. The fact that the P2X-specific purinergic agonist ($\alpha\beta$meATP) failed to elicit $[Ca^{2+}]_i$ in Müller cells in thapsigargin-treated and untreated retinal slices suggests that Müller cells may not express this subtype of purinoceptors. This result, however, should be interpreted with caution, since the P2X receptor channels are known to undergo fast inactivation, and measurements of membrane currents by patch-clamp methods are required to verify this possibility. While retinal neurons have been shown to express P2X2 purinoceptors (Greenwood et al. 1997; Neal and Cunningham 1994), recent studies have shown that Müller cells in adult rat retinae also express P2X purinergic receptors (Neal et al. 1998).

Ca^{2+} waves evoked by purinergic receptors propagate bidirectionally from initiation sites within Müller cell processes. Analysis of Ca^{2+} waves revealed the presence of discrete Ca^{2+} release sites where the magnitude of Ca^{2+} release was significantly higher than in surrounding regions of the cell. Nonuniform distribution of purinergic receptors on Müller cells processes alone could not explain the observation of specialized release sites, but could contribute to wave initiation. Inositol 1,4,5-trisphosphate ($InsP_3$) generated during receptor activation diffuses extremely rapidly in cytoplasm ($D \geq 180$ $\mu m^2/s$) (Allbritton et al. 1992), and any gradient in $InsP_3$ levels will be expected to dissipate rapidly. Wave propagation on the other hand occurs at rates of up to 40 μm/s. In theory, localized patches of purinergic receptors on Müller cell processes together with focal release of agonists could elicit localized wave initiation. Whether such an arrangement exists in the retina needs to be investigated. The regenerative nature of wave propagation that we observed, however, suggests specialized Ca^{2+} release sites along Müller cell processes where Ca^{2+} release function is enhanced.

The phenomenon of specialized Ca^{2+} release sites is remarkably similar to observations in cultured glial cells of the astrocytic and oligodendrocyte lineages (Simpson et al. 1997; Yagodin et al. 1994). The specialized Ca^{2+} release sites serve as wave amplification sites, and mathematical models have provided evidence that they might behave as partially coupled cellular oscillators being coupled by the diffusing Ca^{2+} ions (Li and Rinzel 1994; Roth et al. 1995). We and others have shown that wave amplification sites are endowed with a number of structural specializations, including high-density patches of IP_3Rs, sarcoendoplasmic reticulum Ca^{2+} pumps (SERCA), beadlike concentration of intraluminal calreticulin, and close apposition with one or more mitochondria (Rizzuto et al. 1998; Simpson and Russell 1996). Indeed, fluorescence-based immunocytochemistry of IP_3Rs in Müller cells in retinal slices revealed beadlike staining along processes (data not shown). Thus it is likely that cellular specializations similar to what has been shown in cultured glial cells (Simpson et al. 1997) may support the enhanced local Ca^{2+} release observed in Müller cells in situ.

We found that a majority of Ca^{2+} waves started at the end-feet, or at the apical end of Müller cells and propagated toward cell bodies. This observation is different from results obtained in isolated dispersed tiger salamander Müller cells, where wave initiation sites were most often observed in the apical region (Keirstead and Miller 1997). This may be due to differences in the analysis paradigm, species differences, or possible damage to cells during the dissociation procedure (Newman 1993). We observed many sites of wave initiation in any given cell, where a Ca^{2+} response begins before the arrival of a wave propagated from other areas of the cell. Multiple wave initiation may be explained by patchy distribution of agonist receptors on the cell membrane, the amount of second messenger formed locally in relation to the internal cell vol-

ume, high-density local patches of IP_3Rs, or a lower threshold for activation of IP_3Rs in local regions of the cell. Without adequate receptor distribution studies, it is difficult to differentiate these and other possibilities.

There is strong experimental evidence in both the peripheral and central nervous systems that suggests that ATP released from synaptic terminals participates in modulation of synaptic plasticity (Burnstock 1990; Edwards et al. 1992; Illes and Norenberg 1993; Sawynok et al. 1993). Similarly, ATP released from glial cells has also been shown to elicit glial Ca^{2+} signals that propagate both within cells and between cells in vitro (Cotrina et al. 2000; Guthrie et al. 1999). ATP is one of the several different neurotransmitters present in the retina, and indirect evidence suggests that ATP could be co-secreted with acetylcholine in rabbit retina (Neal and Cunningham 1994). It is not clear what role such purinergic activation of Müller cells plays in modulating activity of retinal neural networks. Furthermore, the primary source of ATP release is not clearly understood. Our results show that ATP is an important signaling molecule in the retinal Müller cells, while adrenergic and glutamatergic agonists were much less efficacious. In a recent study, Newman and Zahs (1997) showed that initiation of Ca^{2+} waves in Müller cells by mechanical stimulation alters excitability of ganglion cells in the vicinity of the wave. This observation, taken together with studies in other brain regions (Duffy and MacVicar 1995; Grosche et al. 1999; Porter and McCarthy 1996), strongly suggests that Ca^{2+}-based excitability in glial cells may have important implications for excitability of neighboring neuronal circuits. Our present study clearly demonstrates that retinal Müller cells possess Ca^{2+}-based excitability similar to glial cells in other brain regions. In addition, we show that cellular mechanisms supporting regenerative wave propagation are remarkably similar in Müller cells in situ and in cultured glial cells and suggest a role for Müller cells in modulating signaling through the retina.

We thank Dr. Laurel Haak for critical reading of the manuscript and Dr. Michael Yvonne for discussions on the retinal preparation.

Present address of Y. Li: Dept. of Pharmacology, Uniformed Services University of Health Sciences, 4301 Jones Bridge Rd., Bethesda, MD 20014.

REFERENCES

ALLBRITTON NL, MEYER T, AND STREYER L. Range of messenger action of calcium ion and inositol 1,4,5-trisphosphate. *Science* 258: 1812–1815, 1992.

BURNSTOCK G. Overview. Purinergic mechanisms. *Annu Rev NY Acad Sci* 603: 1–17, 1990.

BURNSTOCK G. The past, present and future of purine nucleotides as signalling molecules. *Neuropharmacology* 36: 1127–1139, 1997.

BURNSTOCK G, CUSACK NJ, HILLS JM, MACKENZIE I, AND MEGHJI P. Studies on the stereoselectivity of the P2-purinoceptor. *Br J Pharmacol* 79: 907–913, 1983.

COLEMAN PA AND MILLER RF. Measurement of passive membrane parameters with whole-cell recording from neurons in the intact amphibian retina. *J Neurophysiol* 61: 218–230, 1989.

COTRINA ML, LIN JH, LOPEZ-GARCIA JC, NAUS CC, AND NEDERGAARD M. ATP-mediated glia signaling. *J Neurosci* 20: 2835–2844, 2000.

CUSACK NJ AND HOURANI SM. Specific but noncompetitive inhibition by 2-alkylthio analogues of adenosine 5′-monophosphate and adenosine 5′-triphosphate of human platelet aggregation induced by adenosine 5′-diphosphate. *Br J Pharmacol* 75: 397–400, 1982.

DANI JW, CHERNJAVSKY A, AND SMITH SJ. Neuronal activity triggers calcium waves in hippocampal astrocyte networks. *Neuron* 8: 429–440, 1992.

DIXON CJ. Evidence that 2-methylthioATP and 2-methythioADP are both agonists at the rat hepatocyte $P2Y_1$ receptor. *Br J Pharmacol* 130: 664–668, 2000.

DUFFY S AND MACVICAR BA. Adrenergic calcium signaling in astrocyte networks within the hippocampal slice. *J Neurosci* 15: 5535–5550, 1995.

EDWARDS FA, GIBB AJ, AND COLQUHOUN D. ATP receptor-mediated synaptic currents in the central nervous system [see comments]. *Nature* 359: 144–147, 1992.

GOTTESMAN J AND MILLER RF. Pharmacological properties of *N*-methyl-D-aspartate receptors on ganglion cells of an amphibian retina. *J Neurophysiol* 68: 596–604, 1992.

GREENWOOD D, YAO WP, AND HOUSLEY GD. Expression of the P2X2 receptor subunit of the ATP-gated ion channel in the retina. *Neuroreport* 8: 1083–1088, 1997.

GROSCHE J, MATYASH V, MÖLLER T, VERKHRATSKY A, REICHENBACH A, AND KETTENMANN H. Microdomains for neuron-glia interaction: parallel fiber signaling to Bergmann glial cells. *Nature Neurosci* 2: 139–143, 1999.

GUTHRIE PB, KNAPPENBERGER J, SEGAL M, BENNETT MV, CHARLES AC, AND KATER SB. ATP released from astrocytes mediates glial calcium waves. *J Neurosci* 19: 520–528, 1999.

ILLES P AND NORENBERG W. Neuronal ATP receptors and their mechanism of action. *Trends Pharmacol Sci* 14: 50–54, 1993.

KEIRSTEAD SA AND MILLER RF. Calcium waves in dissociated retinal glial (Muller) cells are evoked by release of calcium from intracellular stores. *Glia* 14: 14–22, 1995.

KEIRSTEAD SA AND MILLER RF. Metabotropic glutamate receptor agonists evoke calcium waves in isolated Müller cells. *Glia* 21: 194–203, 1997.

LI YX AND RINZEL J. Equations for InsP3 receptor-mediated $[Ca^{2+}]_i$ oscillations derived from a detailed kinetic model, a Hodgkin-Huxley like formalism. *J Theor Biol* 166: 461–473, 1994.

LLINAS RR. Calcium in synaptic transmission. *Sci Am* 247: 56–65, 1982.

MENNERICK S AND ZORUMSKI CF. Glial contributions to excitatory neurotransmission in cultured hippocampal cells. *Nature* 368: 59–62, 1994.

NEAL M AND CUNNINGHAM J. Modulation by endogenous ATP of the light-evoked release of ACh from retinal cholinergic neurones. *Br J Pharmacol* 113: 1085–1087, 1994.

NEAL MJ, CUNNINGHAM JR, AND DENT Z. Modulation of extracellular GABA levels in the retina by activation of glial P2X-purinoceptors. *Br J Pharmacol* 124: 317–322, 1998.

NEDERGAARD M. Direct signaling from astrocytes to neurons in cultures of mammalian brain cells. *Science* 263: 1768–1771, 1994.

NEWMAN E AND REICHENBACH A. The Muller cell, a functional element of the retina. *Trends Neurosci* 19: 307–312, 1996.

NEWMAN EA. Inward-rectifying potassium channels in retinal glial (Müller) cells. *J Neurosci* 13: 3333–3345, 1993.

NEWMAN EA AND ZAHS KR. Calcium waves in retinal glial cells. *Science* 275: 844–847, 1997.

NEWMAN EA AND ZAHS KR. Modulation of neuronal activity by glial cells in the retina. *J Neurosci* 18: 4022–4028, 1998.

NORTH RA AND BARNARD EA. Nucleotide receptors. *Curr Opin Neurobiol* 7: 346–357, 1997.

PASTI L, VOLTERRA A, POZZAN T, AND CARMIGNOTO G. Intracellular calcium oscillations in astrocytes, a highly plastic, bidirectional form of communication between neurons and astrocytes in situ. *J Neurosci* 17: 7817–7830, 1997.

PORTER JT AND MCCARTHY KD. Hippocampal astrocytes in situ respond to glutamate released from synaptic terminals. *J Neurosci* 16: 5073–5081, 1996.

RIZZUTO R, PINTON P, CARRINGTON W, FAY FS, FOGARTY KE, LIFSHITZ LM, TUFT RA, AND POZZAN T. Close contacts with the endoplasmic reticulum as determinants of mitochondrial Ca^{2+} responses. *Science* 280: 1763–1766, 1998.

ROTH BJ, YAGODIN SV, HOLTZCLAW L, AND RUSSELL JT. A mathematical model of agonist-induced propagation of calcium waves in astrocytes. *Cell Calcium* 17: 53–64, 1995.

SAWYNOK J, DOWNIE JW, REID AR, CAHILL CM, AND WHITE TD. ATP release from dorsal spinal cord synaptosomes, characterization and neuronal origin. *Brain Res* 610: 32–38, 1993.

SIMPSON PB, MEHOTRA S, LANGE GD, AND RUSSELL JT. High density distribution of endoplasmic reticulum proteins and mitochondria at specialized Ca^{2+} release sites in oligodendrocyte processes. *J Biol Chem* 272: 22654–22661, 1997.

SIMPSON PB AND RUSSELL JT. Mitochondria support inositol 1,4,5-trisphosphate–mediated Ca^{2+} waves in cultured oligodendrocytes. *J Biol Chem* 271: 33493–33501, 1996.

SIMPSON PB AND RUSSELL JT. Mitochondrial Ca^{2+} uptake and release influence metabotropic and ionotropic cytosolic Ca^{2+} responses in rat oligodendrocyte progenitors. *J Physiol (Lond)* 508: 413–426, 1998.

SMITH SJ. Do astrocytes process neural information? *Prog Brain Res* 94: 119–136, 1992.

THASTRUP O. Role of Ca2(+)-ATPases in regulation of cellular Ca^{2+} signalling, as studied with the selective microsomal Ca2(+)-ATPase inhibitor, thapsigargin. *Agents Actions* 29: 8–15, 1990.

WU RL AND BARISH ME. Astroglial modulation of transient potassium current development in cultured mouse hippocampal neurons. *J Neurosci* 14: 1677–1687, 1994.

YAGODIN SV, HOLTZCLAW L, SHEPPARD CA, AND RUSSELL JT. Nonlinear propagation of agonist-induced cytoplasmic calcium waves in single astrocytes. *J Neurobiol* 25: 265–280, 1994.

ZAHS KR AND NEWMAN EA. Asymmetric gap junctional coupling between glial cells in the rat retina. *Glia* 20: 10–22, 1997.